JOURNAL OF GEOPHYSICAL RESEARCH, VOL. 113, A04307, doi:10.1029/2007JA012739, 2008

Ozone diurnal variations and mean profiles in the mesosphere, lower thermosphere, and stratosphere, based on measurements from SABER on TIMED

Frank T. Huang,[1] Hans G. Mayr,[2] James M. Russell III,[3] Martin G. Mlynczak,[4] and Carl A. Reber[5]

Received 19 August 2007; revised 13 December 2007; accepted 11 January 2008; published 24 April 2008.

[1] Ozone measurements from SABER on the TIMED satellite form a unique data set. They provide global information over the range of local solar times, from the lower stratosphere into the lower thermosphere, from the beginning of 2002, by one instrument. On the basis of zonal means of these data, we present new results from 20 to 100 km in altitude and from 48°S to 48°N in latitude, of ozone diurnal variations over 24 h in local solar time and over an annual cycle. While some of the results are new for the stratosphere, such comprehensive results for the mesosphere and lower thermosphere have not been available before. The diurnal variations generally become increasingly significant from the upper stratosphere into the lower thermosphere and provide information on the photochemistry of ozone and effects of transport over a diurnal cycle. Over most altitudes in the mesosphere and lower thermosphere (MLT), our estimates show the expected decrease in ozone after sunrise, with smaller variations during the day, and the increase near sunset. Outside of a small altitude near 80 km, the nighttime mixing ratios are generally larger than the daytime values. The diurnal variations themselves appear to exhibit variations over an annual cycle, including semiannual and annual variations. We compare the SABER results with data obtained about 10 years earlier by the MLS instrument on UARS, and with results by others based on data from HRDI on UARS, from the Solar Mesosphere Explorer (SME), from selected space shuttle experiments, and from ground-based measurements. From the middle mesosphere to higher altitudes, departures from local thermodynamic equilibrium (non-LTE) can be significant, and the uncertainties can be larger than those at lower altitudes.

Citation: Huang, F. T., H. G. Mayr, J. M. Russell III, M. G. Mlynczak, and C. A. Reber (2008), Ozone diurnal variations and mean profiles in the mesosphere, lower thermosphere, and stratosphere, based on measurements from SABER on TIMED, *J. Geophys. Res.*, *113*, A04307, doi:10.1029/2007JA012739.

1. Introduction

[2] We present results based on ozone measurements from the Sounding of the Atmosphere using Broadband Emission Radiometry (SABER) instrument [*Russell et al.*, 1999] on the Thermosphere-Ionosphere-Mesosphere-Energetics and Dynamics (TIMED) satellite, and from the Microwave Limb Sounder (MLS) [*Barth et al.*, 1983] on the Upper Atmosphere Research Satellite (UARS) [*Reber*, 1993]. The importance of atmospheric ozone from both a practical and scientific view is well known. Understanding the global diurnal variations provides important information on the photochemistry, dynamics and transport, and energetics of the atmosphere. Ozone measurements from SABER are unique in the breadth of their information content. Measurements are made over the globe from about 15 to 100 km, over 24 h in local solar time (LST), and over multiple years, since the beginning of 2002. This kind of information has not been available previously, especially from one instrument. Although SABER and UARS measurements provide information over the full range of local times, the measurements are still asynoptic, and the analysis is not straightforward, as discussed in section 2. Nevertheless, SABER and MLS data provide the potential to realistically estimate both global diurnal variations and their variations over an annual cycle that data from other sources do not provide.

[3] We have derived diurnal variations based on zonal means of SABER ozone mixing ratio data from 20 km to 100 km, 48°S to 48°N latitude, and 0 to 24 h local solar

[1]Creative Computing Solutions Inc., Rockville, Maryland, USA.
[2]NASA Goddard Space Flight Center, Greenbelt, Maryland, USA.
[3]Center for Atmospheric Sciences, Hampton University, Hampton, Virginia, USA.
[4]NASA Langley Research Center, Hampton, Virginia, USA.
[5]Science and Technology Corporation, Hampton, Virginia, USA.

0148-0227/08/2007JA012739$09.00

time, for years 2002 through 2005, and from MLS for 1992 into1994. These results are the first to cover such a wide temporal and spatial range, over 24 h of local solar time. While much of the results are new for the stratosphere, such comprehensive results for the mesosphere and lower thermosphere (MLT) have not been available before.

[4] In section 2 we review the data characteristics and analysis, and the special sampling characteristics of SABER (MLS) in local time. In section 3 we discuss the data quality in relation to some previous data, and in section 4 we present our results.

2. Data Sampling, and Analysis

[5] Our results are derived from version 1.06 of SABER level 2A data, which are provided by the SABER project for years 2002 through 2005. The SABER instrument [*Russell et al.*, 1999] views the Earth's limb to the side of the orbital plane, and ozone emissions in the 9.6 μm band are used to retrieve the mixing ratios, corresponding to the line-of-sight tangent point. The spacecraft makes $\sim$15 orbits per day at an orbital inclination of $\sim$74°. To obtain profiles, once every 58 s, SABER scans up and down the Earth's horizon collecting data over an altitude range of approximately 180 kilometers. The north-south motion of the satellite covers the different latitudes ($\sim$4° between profiles at low latitudes), and the range of longitudes ($\sim$25° between orbits) are covered over one day due to the rotation of the earth. The data are interpolated to 4° latitude intervals and 2.5 km altitude intervals from 20 to 100 km, and for each day averaged over longitude for analysis.

[6] Although SABER on TIMED and MLS on UARS sample over the range of local times, they need 60 and 36 days respectively, to do so. Over a given day and for a given latitude circle, measurements are made as the satellite travels northward (ascending mode) and again as the satellite travels southward (descending mode). Data at different longitudes are sampled over one day as the Earth rotates relative to the orbit. The orbital characteristics of the satellite are such that over a given day, for a given latitude circle, and a given orbital mode (ascending or descending), the local time at which the data are measured are essentially the same, independent of longitude and time of day. For a given day, latitude, and altitude, if we work with data averaged over longitude, we get 2 averages, one for the ascending orbital mode and one for the descending mode, each corresponding to a different local solar time. Each can be biased by the local time variations, and is therefore not a true zonal mean. True zonal means are averages made at a specific time (not over a day) over longitude around a latitude circle, with the local solar time varying by 24 h over 360° in longitude. The local times of the SABER measurements decrease by about 12 min from day to day, and it takes 60 days to sample over the 24 h of local time. Although this provides essential information in local time, over 60 days, variations can be due to both local time and other variables, such as season. Diurnal and mean variations are embedded together in the data, and need to be unraveled from each other to obtain more accurate estimates of each.

[7] Our algorithm is designed for this type of sampling in local time, and provides estimates of both diurnal and mean variations together in a consistent manner. It attempts to remove the bias in the mean due to the local time. At a given latitude and altitude for data over a period of a year, the algorithm performs a least squares estimate of a two-dimensional Fourier series where the independent variables are local solar time and day of year, and variations as a function of local time and mean variations (e.g., semiannual oscillations, SAO) over one year are generated. Results for the mean variations of ozone such as the SAO and quasi-biennial oscillations (QBO) are given in a companion paper [*Huang et al.*, 2008]. We currently do not generate results poleward of 48° latitude because data exist at higher latitudes only on alternate yaw intervals (60 days). Because it takes SABER 60 days (36 days for MLS) to sample over the range of local times, the information of seasonal variations of the diurnal variations themselves may be limited, and we limit the number of coefficients estimated as described in the Appendix.

[8] Once the coefficients are estimated, both the mean components and the diurnal variations can be calculated directly for any day of year. The algorithm (given in the Appendix) has been applied previously to SABER temperature measurements of diurnal variations (thermal tides) and mean variations to study intraseasonal (ISO), semiannual (SAO), and quasi-biennial (QBO) variations [*Huang et al.*, 2006a, 2006b, 2006c]. It has also been successfully applied to wind measurements from the TIMED Doppler Interferometer (TIDI), as described by *Huang et al.* [2006a], and to MLS ozone measurements [*Huang et al.*, 1997].

[9] Figure 1 shows an example of the sampling properties of SABER data and how well our algorithm estimates the data. SABER ozone mixing ratio (parts per million by volume, ppmv) data, averaged over longitude, at the Equator and 90 km altitude, are plotted versus day for year 2005. For a given day, the solid and dashed lines represent the data averaged over longitude from the ascending (satellite going northward) and descending modes, respectively, each corresponding to one local time. As can be seen, the two data points for each day can differ by up to several ppmv, reflecting different local times. The local times decrease by about 12 min from day to day. The diamonds and squares depict our estimates, evaluated at the same day and same local time as the data. As can be seen, the estimates approximate the measurements reasonably, although there are some intervals over several days where our estimates do not follow the data as well, so some smoothing exists. At 90 km, the amplitudes of diurnal variations are larger than those at lower altitudes, with the nighttime values being up to an order of magnitude larger than daytime values, thereby testing the algorithm more than at lower altitudes. We note that Figure 1, as well as Figures 2 and 3 are taken from the companion paper [*Huang et al.*, 2008] noted earlier.

3. Data Quality and Previous Measurements

3.1. Previous Measurements

[10] In past decades, satellite-borne instruments have provided invaluable global measurements of ozone. The preponderance of the measurements has been made in the stratosphere and below, where diurnal variations are relatively small, and there has been a lack of measurements in

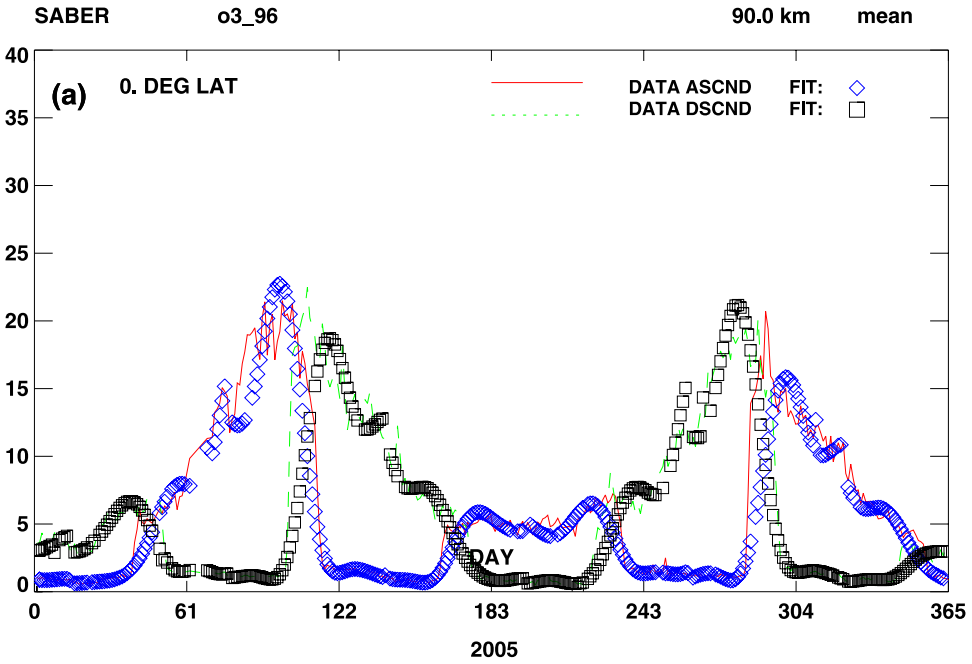

Figure 1. Zonally averaged SABER ozone data (ppmv) and estimated results plotted versus day of year for 2005, at the Equator and 90 km. Solid line and diamonds represent ascending mode data and fit, respectively. Dashed line and squares represent descending mode data and fit, respectively.

the mesosphere and above, where diurnal variations can be dominant.

[11] Unlike TIMED and UARS, the orbital characteristics of other satellites, and/or the length of their missions (e.g., space shuttle missions), are such that the local solar times at which the data are taken are limited. Most satellite orbits are sun-synchronous, so that the local times at which measurements are made do not change from day to day, and remain the same for the duration of the mission. In these cases, when diurnal variations are not negligible, it is impractical to quantitatively analyze the measurements for their behavior as a function of local time and to estimate unbiased zonal mean values. Examples of other satellites that sound the atmosphere to obtain ozone profiles include the Solar

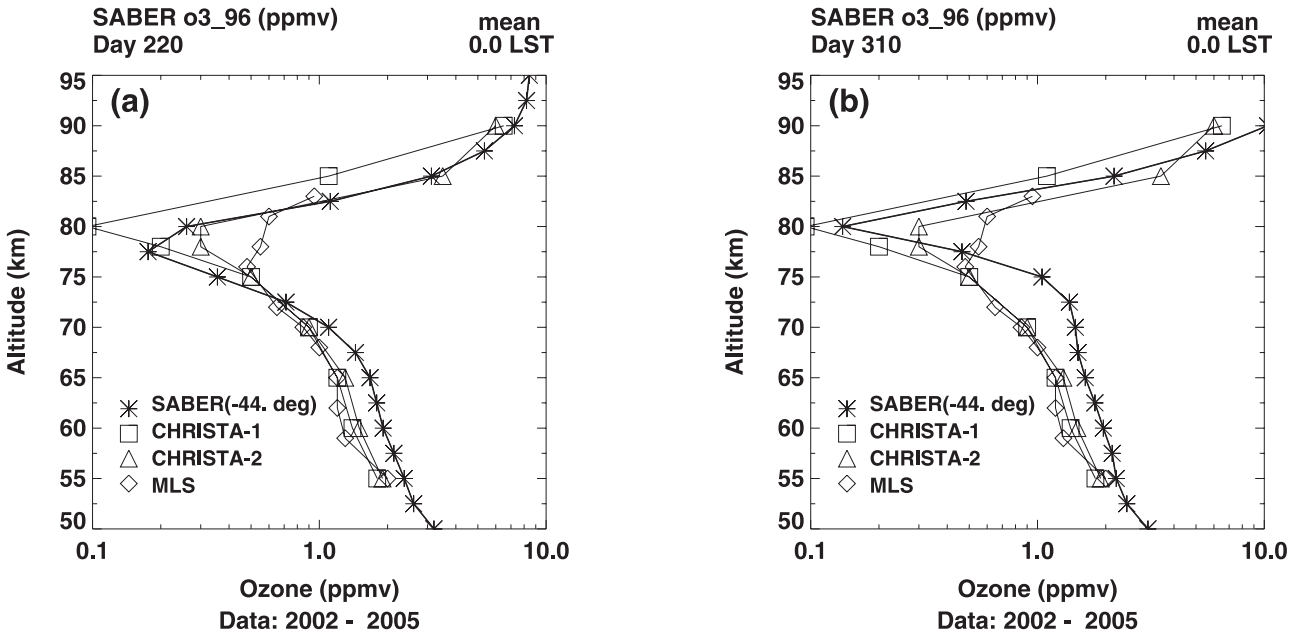

Figure 2. Our derived results (asterisks, 44°S latitude, 0 h LST), CRISTA-1 (squares: mean of 120 profiles, 4–12 November 1994, 40–55°S latitude, 23-3 h LST), CRISTA-2 (triangles: mean of 17 profiles, 8–16 August 1997, 40–55°S latitude, 23-3 h LST), and MLS (diamonds, August, 1992, 40–55°S latitude, 23-3 h LST) results on altitude versus ozone coordinates. For our results, the left plot is for day 220 (8 August) and the right plot is for day 310 (6 November). Left and right plots contain same data for CRISTA-1, CRISTA-2, and MLS.

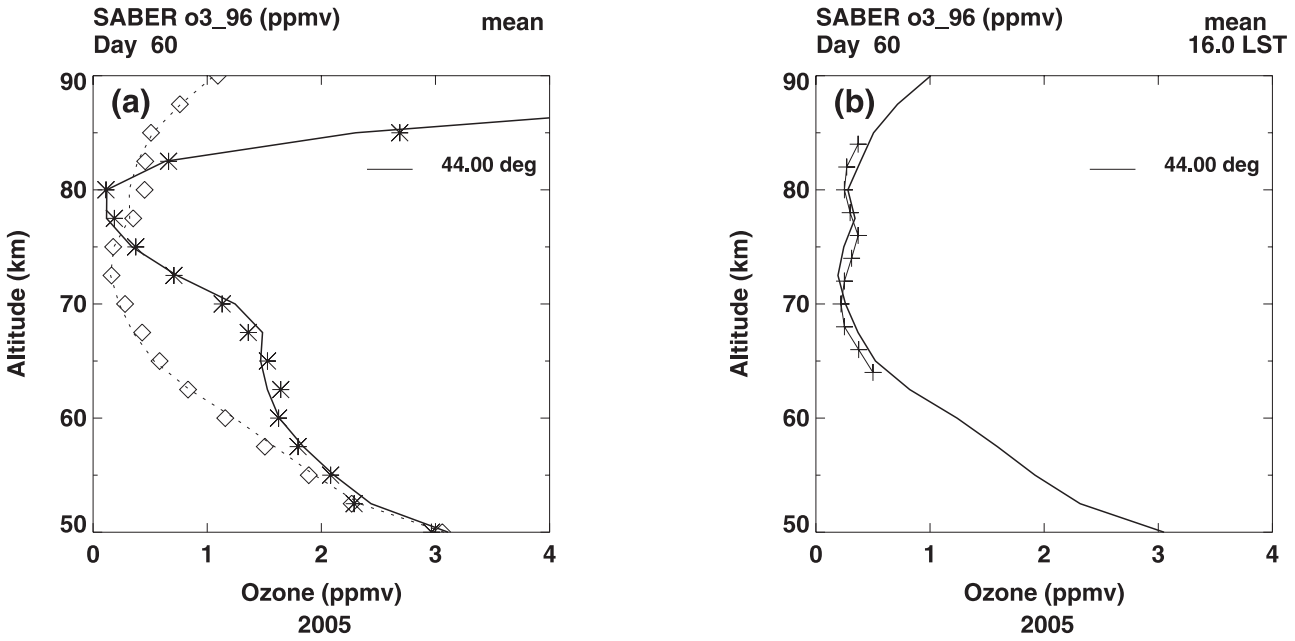

Figure 3. Altitude versus zonal mean ozone mixing ratios (ppmv). Left (a) zonal mean of SABER data for year day 2005060; asterisks: ascending mode data (~2 h LST), diamonds: descending mode data (~17 hours LST); lines: our derived estimates. Right (b): '+'s: SME data at 45°N latitude for March, ~16 h local time; line: our estimates at 16 h local time, based on SABER data for year day 2005060.

Mesosphere Explorer (SME) [*Barth et al.*, 1983], the Nimbus satellites, the Earth Observing System (EOS) satellites, the NOAA polar orbiters, and selected space shuttle missions [e.g., *Kaufmann et al.*, 2003]. Measurements from these satellites do not provide the sampling needed to quantitatively analyze variations over the 24 h of local times. For example, the ozone measurements made by SME are all made essentially at one local time (~16 h), irrespective of longitude and day. The Halogen Occultation Experiment (HALOE) on UARS measures ozone only during sunset and sunrise. *Ricaud et al.* [1996] have presented diurnal variations of ozone based on MLS on UARS for some sample cases. They note, as we did earlier, that if there are trends in the 36 days it takes to sample the data over the range of local times, then changes in ozone may well be induced more by monthly variations than by diurnal effects in the sampled data. They therefore restricted their analysis to altitudes from about 55 to 70 km, where the diurnal variations are larger than 10% of the diurnal average. *Wu and Jiang* [2005] have analyzed ozone and temperature data from a more recent version of UARS MLS data, but their results do not contain the details needed for comparison. *Marsh et al.* [2002] provide mesospheric daytime ozone measurements derived from HRDI measurements on UARS.

[12] Over the decades, ground based measurements [e.g., *Schneider et al.*, 2005; *Zommerfelds et al.*, 1989; *Connor et al.*, 1994] have provided ozone and temperature measurements as a function of local time with good time resolution, from about 25 to 75 km, but do not provide good global coverage.

3.2. Data Quality

[13] From the middle mesosphere to higher altitudes, departures from local thermodynamic equilibrium (non-LTE) can be significant, complicating the retrieval of ozone mixing ratios, and the uncertainties can be larger than those at lower altitudes. At these higher altitudes, the SABER ozone mixing-ratios may be systematically overestimated. See the discussion in reference to Figure 2, below. The systematic uncertainties (accuracy) can be due to instrument characterization and the retrieval of mixing ratios (inversion of the radiative transfer models), among other things. Examples of instrument characterization include radiometric and field-of-view calibrations.

[14] In the final analysis, validation depends on comparisons with "ground truth". However, there is a clear lack of correlative measurements in the mesosphere and lower thermosphere (MLT). This situation is exacerbated by diurnal variations of ozone, which can be several times larger at night compared to daylight. If correlative measurements are not available at both the same time, especially local solar time, and location, discrepancies can be relatively large and the causes difficult to pin down. As discussed below, for the upper mesosphere and lower thermosphere, it is currently difficult to reach definite conclusions in comparing with past measurements.

[15] Of the data sources mentioned above, the more relevant ones are the Cryogenic Infrared Spectrometers and Telescopes for the Atmosphere (CRISTA), [*Kaufmann et al.*, 2003] and the Solar Mesosphere Explorer (SME), [*Thomas*, 1990; *Barth et al.*, 1983]. CRISTA was flown on two space shuttle missions in November 1994 (CRISTA-1) and August 1997 (CRISTA-2), each with measurements lasting a little more than one week, from 50 to 95 km. The short duration resulted in limited sampling over local time, and results were given at selected daytimes and nighttimes. The SME provided ozone measurements from about 50 to near 90 km, but only at ~16 h local time. Additional measurements are provided by ground-based radiometers

[e.g., *Zommerfelds et al.*, 1989; *Connor et al.*, 1994; *Schneider et al.*, 2005]. The sampling and resolution in local time is a better, but the spatial coverage is limited and the altitude resolution is not as good that of CRISTA or SME.

[16] Figure 2 shows our results along with those of *Kaufmann et al.* [2003], transcribed by us from their Figure 13a, which show CRISTA-1 and CRISTA-2 results, plus UARS MLS (also from *Kaufmann et al.* [2003]) data. The asterisks depict the SABER results. The left plot is for day 220 (8 August) and the right plot is for day 310 (6 November). The left and right plots contain the same data for CRISTA-1, CRISTA-2, and MLS. Squares denote CRISTA-1 results, triangles denote CRISTA-2, and diamonds show MLS results, on altitude versus ozone coordinates (semi-log).

[17] As noted earlier, the uncertainties of ozone measurements in the MLT can be relatively large. *Kaufmann et al.* [2003] report that the CRISTA-1 and CRISTA-2 systematic errors in the mesosphere can be as large as 40%. In their comparison with HRDI and MLS, below the ozone minimum (~75 km), the CRISTA, HRDI, and MLS profiles differ by less than 30%, usually less than their individual uncertainties. However, near 75 km and above, the systematic errors and standard deviations can be much larger. As *Kaufmann et al.* [2003] state, ''the two CRISTA profiles agree well below 75 km, but above this altitude the CRISTA-2 profile is higher by up to a factor of 5''. Comparisons with MLS are also not good at these altitudes, and cannot be reconciled by uncertainties in CRISTA and MLS results, which together can exceed 100%.

[18] *Zommerfelds et al.* [1989] have compared their ground-based ozone measurements with SME data from about 50 to 75 km. They compared data for December and April, although not in the same years. For April, they state that with the exception of their value near 68 km, error bars for the two profiles generally overlap. *Zommerfelds et al.* [1989] state ''the retrievals for December show more substantial disagreement not only in absolute values for mixing ratios but for the general shape of the vertical profiles''. *Marsh et al.* [2002] provide mesospheric daytime ozone measurements derived from HRDI measurements on UARS. The upper limits of the standard deviations and systematic errors appear to approach 50%, and they note that SME systematic uncertainties are comparable, while SME random errors are ~10% below 80 km and 20% near 90 km.

[19] For more current ozone measurements, we note the MLS instrument on the Aura satellite (MLS-Aura), which is sun synchronous and measures at only two local times, one ~1.45 pm for the ascending mode, and one at nighttime, for the descending mode. The MLS-Aura project [*Froidevaux et al.*, 2007] recommends using their data (v2.2) from 215 hPa to 0.02 hPa (~75 km), but not at higher altitudes. Near 75 km, the systematic error (accuracy) is ~35% with increasing uncertainties at higher altitudes, and these are then in line with other data uncertainties discussed earlier. They have compared with data from the stratosphere aerosol and gas experiment (SAGE-II) instrument on the Earth radiation budget satellite (ERBS) and the halogen occultation experiment (HALOE) on UARS. Below ~50 km, the differences with HALOE are ~5% to 10% or less, and increase to ~30% near 60km, with the trend in uncertainties rising with altitude. The comparisons with SAGE II in the stratosphere are very good (generally to within a few percent), show differences from 5% to 10% near 50 km, and increase to ~20% near 60km. The trend in uncertainties increases with altitude above ~50 km, and if extrapolated, the differences would be appear to be greater than 40% above 60 km, again in line with uncertainties from other measurements mentioned earlier. The quality of MLS-Aura ozone data is supported even at higher altitudes by ground-based microwave radiometer measurements from ~20 to 72 km [*Boyd et al.*, 2007]. The comparisons are generally excellent, being within 5% from about 26 to 70 km, and up to ~13% at other altitudes.

[20] The magnitudes of uncertainties for the current data version of SABER ozone are comparable to the above estimates for CRISTA, SME, MLS, and HRDI. The difficulties in reaching conclusions are evident, as the comparisons are tenuous. In addition, our focus here is diurnal variations over the full 24 h of local time, and there are no comparable previous ozone results with which to compare, and an estimate of uncertainties would not in itself validate the results. However, the ozone diurnal variations are relative to a mean state and they should be more robust, as this mitigates the effect of systematic errors.

[21] Our approach here is to examine sensitivity to relative variations in the data, and to analyze the expected correlations between ozone and temperature. The first example can be seen from the left plot of Figure 3a, which shows SABER ozone data zonally averaged separately for ascending and descending modes, year day 2005060, versus altitude. The asterisks correspond to ascending mode data at ~2 h local time, and diamonds denote descending mode data at ~17 h. The lines denote our derived estimates evaluated at those local times for the same day. As can be seen, with the exception of a narrow altitude interval near 80 km, the mean daytime ozone mixing ratios are generally smaller than the values at night. Importantly, this is consistent with the ROSE model [*Smith*, 2004, Figure 4], where the mean daytime values are larger than the mean nighttime values only near 80 km. This helps verify the precision of relative variations in the measurements. The right plot of Figure 3b corresponds to the left plot but shows our estimates (line) at 16 h local time and 44°N latitude, and the '+'s denote SME results (for March, data from 1981 to 1986, 45°N latitude) that we transcribed from *Thomas* [1990, Figure 3c]. The graphs of *Thomas* [1990] are in units of pressure, so there may be a small vertical shift relative to our results. Ironically, this better-than-expected comparison is probably fortuitous because the systematic uncertainties are significantly larger. What is more significant is the ''bulge'' between 75 and 80 km in both of our results, and the relatively small amplitudes of the bulge support the sensitivity of the agreement. The bulges are a systematic feature of the SME data, and have been noted by *Bevilacqua et al.* [1990], *Marsh and Smith* [2003], and *Zommerfelds et al.* [1989]. Although it is not our intent here to interpret the physics of the bulge, but to study it in terms of the validity of our results, we believe that the bulge may well be due to the local time at which data were taken, and is a reflection of ozone diurnal variations. Our results also show that, averaged over local time, the bulges are no longer apparent, indicating that the

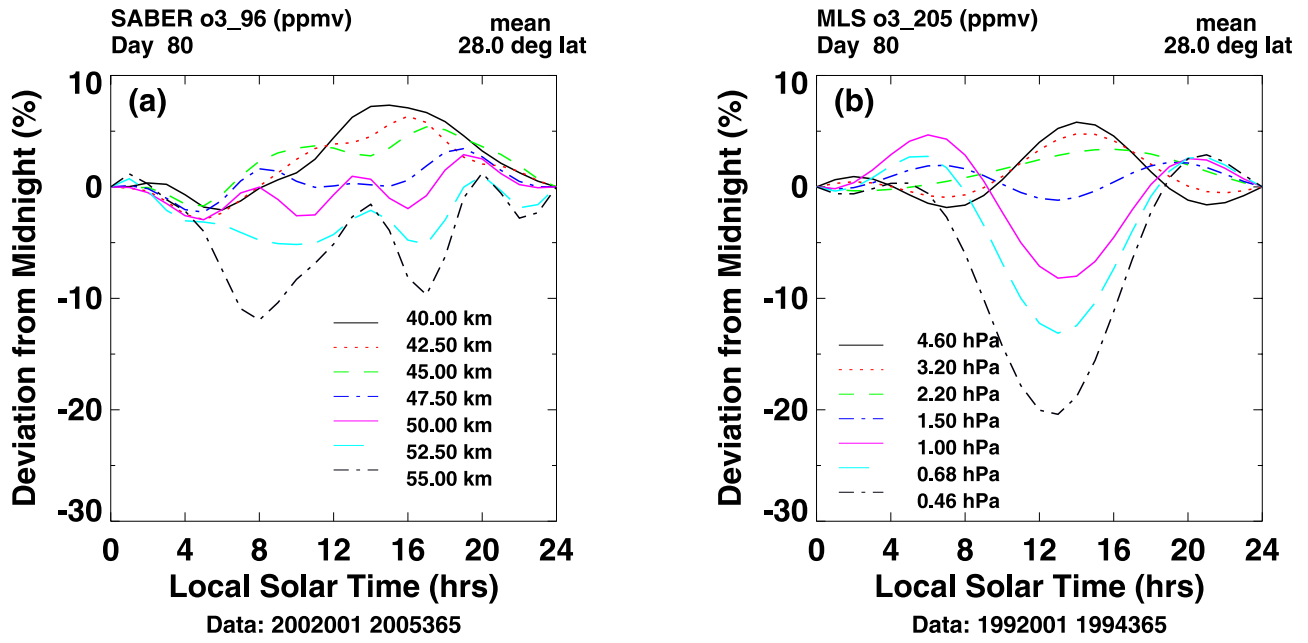

Figure 4. Left (a): Percent deviation from midnight value of ozone mixing ratios (ppmv) for day 80, 28°N, as a function of local solar time from 40 to 55 km based on SABER data (years 2002–2005). Right (b): corresponds to (a) but based on MLS data (years 1992–1994) from 4.6 to 0.46 hPa (~38 to 55 km).

SME bulges are likely due to the local time at which the data were sampled (~16 h local time). Recall that our results show that only in this altitude interval around 80 km are the ozone daytime mixing ratios larger than the nighttime values.

[22] This explanation of the SME bulge also attests to the validity of SABER data. The likelihood of (1) the bulges being in both the SME and in our results near 80 km, (2) the ozone daytime concentration being larger than the nighttime concentration only near 80 km, and (3) the agreement of (2) with the ROSE model all being coincidental is obviously low. In addition, our results show that the diurnal variations themselves follow a semi-annual variation, which is consistent with the reported semi-annual variation of the bulges in the SME data [*Bevilacqua et al.*,1990; *Marsh and Smith*, 2003].

[23] One example where we can compare with independent results is given in Figure 4, which shows our results of zonal mean ozone mixing ratios (ppmv) based on SABER (left (a)) and on MLS (right (b)) data. It gives the percentage deviation from midnight values versus local solar time, at 28°N from 40 to 55 km for SABER and 4.6 hPa to 0.46 hPa (~38 to 55 km) for MLS, chosen to compare with results from the United Kingdom Meteorological Office (UKMO) chemical model [*Huang et al.*, 1997]. The SABER results are based on data from 2002–2005, and the MLS data are from 1992–1994. Of significance is that results derived from SABER and MLS both show a change in regime from larger daytime (compared to midnight) values beginning from 40 km (about 3.2 hPa), to intermediate daytime values near 42.5, 45, 47.5 km (about 3.2, 2.2, 1.5 hPa), to lower daytime values at 50 to 55 km (about 1 to 0.46 hPa). The intermediate values based on SABER and MLS data compare to better than a few percent, and as shown by *Huang et al.* [1997], the UKMO chemical model also agreed quite well with these results. The UKMO model also showed the local maximum in mid afternoon at 55 km in the left plot (a) of Figure 4, but not found in the right plot (b) at 0.46 hPa (~55 km), based on MLS data. This is probably because the results based on MLS data reflects only diurnal and semidiurnal components, while the left plot, using SABER data, reflects twice as many Fourier coefficients in local time. When the UKMO results were restricted to two Fourier components, the local maximum at mid afternoon also disappeared. This lends confidence to both the data results and the model. We have not reevaluated the MLS results using the same number of coefficients as for the SABER data because the MLS level 3B data were not archived, and are no longer available.

[24] As noted earlier, the algorithm estimates variations as a function of local time in conjunction with mean variations such as the ozone and temperature quasi-biennial (QBO) and semiannual oscillations (SAO). Our results for the temperature QBO and SAO are described by *Huang et al.* [2006c], and those for ozone are the subject of a companion paper [*Huang et al.*, 2008]. Although the QBO is not the subject of this study, we give an example in Figure 5 to underscore the validity of SABER data (and the analysis), such as the QBO and the SAO. In the stratosphere, correlations between ozone and temperature measurements were noted by *Finger et al.* [1995], among others, who analyzed ozone data from the Solar Backscatter Ultraviolet Radiometer (SBUV) and temperature data from the National Centers for Environmental Prediction, Climate Prediction Center (NCEP/CPC) taken over more than a decade. Generally, they found an overall positive correlation between ozone and temperature in the lower stratosphere and a mostly negative correlation in the upper stratosphere. On the basis of chemistry, the dependence of reaction rates on temperature leads to a negative correlation between ozone

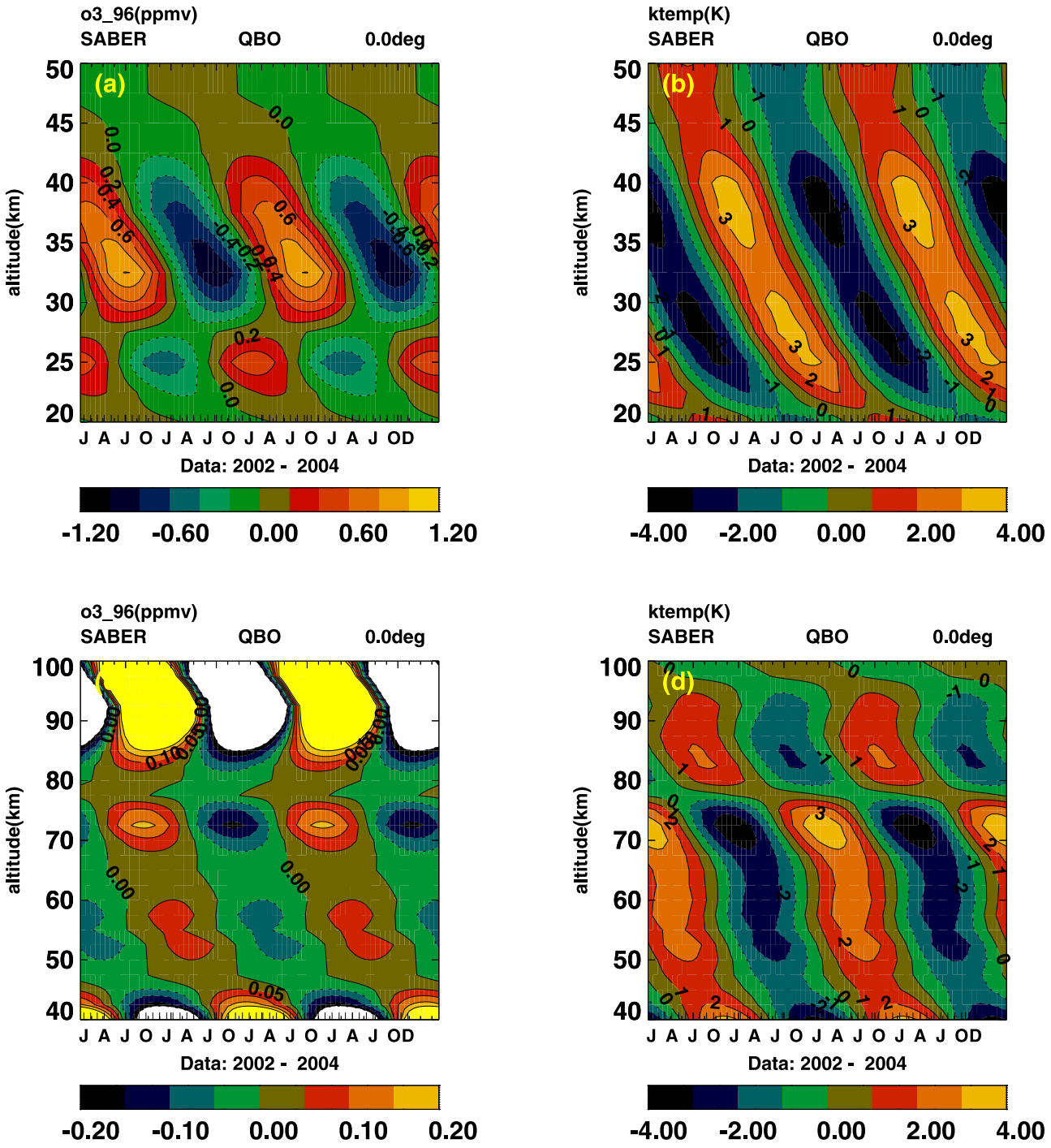

Figure 5. Upper row: QBO results based on SABER ozone (ppmv, left (a)) and temperatures (K, right (b)) at the Equator on altitude (20–50 km)-day coordinates. The plots are over 2 cycles. Contour intervals are 0.2 (top row left) for ozone, and 1 K for temperature. Solid contours denote zero and positive values; dashed lines, negative values. Lower row: corresponds to the upper row, but for 40 and 100 km altitude. The plots are over 2 cycles. In the lower left plot, we have allowed the scales to saturate (near 40 km and above ~85 km) in order to show the smaller values between 45 and 85 km more clearly.

and temperature perturbations. However, *Rood and Douglass* [1985] and *Douglass et al.* [1985] show that dynamics can also cause significant anti-correlations between temperature and ozone, so the situation may not always be simple to interpret. *Brasseur and Solomon* [2005] provide estimates of spatial areas in the atmosphere comparing the relative importance of chemistry versus dynamics for ozone.

[25] For example, Figure 5 shows our derived QBO results based on SABER ozone mixing ratios (left plots, ppmv) and temperatures (right plots, K) at the Equator on altitude versus day coordinates, based on data from year days 2002001 to 2004060, assuming a period of 26 months, with the abscissa plotted over 2 cycles. The upper row of Figure 5 shows results for altitudes between 20 and 50 km. Near 28 km, the

QBO in ozone mixing ratios (left, (a)) undergo relatively sharp changes of phase with altitude. Below about 28 km, the ozone and temperature (right, (b)) are just about in phase with each other as a function of day of year. Above this altitude, the ozone and temperature are mostly out of phase. The rapid changes of phase in ozone near 28 km are consistent with the results given by *Hasebe* [1994], using SAGE II data. *Hollandsworth et al.* [1995] using SBUV data, show a phase shift at 31 km. They attribute the phase shift to the relative importance of dynamics versus chemical control. The lower row of Figure 5 corresponds to upper row but for 40 to100 km altitudes. It can be seen that the ozone and temperatures remain mostly out of phase with increasing altitude up to about 75 km. Between 75 and 80 km, the temperature phases change rapidly with altitude, so that above about 80 km, the ozone and temperature QBOs are again more in phase with respect to day of year.

[26] Because uncertainties due to non-LTE conditions are not significant below the middle mesosphere, in this region, the relative phases between the ozone and temperature in Figure 5 are robust and expected. The probability that the expected phase-relationships extend from the stratosphere into the mesosphere and higher are fortuitous is unlikely, and lends confidence to the SABER data and our derived results at higher altitudes as well.

4. Results

4.1. Mean Profiles and Morphology

[27] Figure 6 shows examples of our derived zonal mean ozone mixing ratios (ppmv) on altitude (20 to 100 km) versus latitude (48°S to 48°N) coordinates, for day 85 (upper row (a, b) and lower left (c)) and day 195 (lower right (d)). The results are based on SABER data from different years (2002–2005) merged into one 365-day period. What makes Figure 6 different from previous plots of this type, aside from the large altitude range, is that it shows our derived zonal mean values that are averages over both local time and longitude in a consistent manner (1a, top left, and 1d, lower right). Previous results based on other satellite data usually correspond to one local time, as in Figures 6b (16 h local time, top right), and 1c (midnight, lower left). The differences are not important in the middle and lower stratosphere, where diurnal variations are relatively small, but become more significant in the upper stratosphere, mesosphere, and higher. It can be seen from Figures 6b and 6c that from the upper stratosphere on up, the nighttime values are mostly larger than daytime values. Over a day, ozone is destroyed via photolysis by solar radiation and by chemical reactions, and is created through recombination of atomic and molecular oxygen. Figures 6a and 6d (for days 85 and 195, near equinox and solstice, respectively) are chosen to show the variations in the zonal mean values with season.

[28] As a function of altitude, qualitatively consistent with past measurements, there are two evident local maximums in Figure 6 at low latitudes, one near 30 km and a second near 95 km. In the middle mesosphere and higher, due to non-LTE considerations, the ozone data may be overestimated (see section 3). The stratospheric maximum near 30 km is well known. For the maximum above 90 km, *Kaufmann et al.* [2003] state that the (expected) equatorial maximum above 90 km was not clearly resolved by the CRISTA data because it is near the maximum altitude of their retrieval, but based on the ROSE model [*Rose and Brasseur*, 1989], the expected maximum is likely because of downward transport of atomic oxygen due to atmospheric tides, and the latitudinal distribution is also strongly biased by thermal tides.

[29] Not as discernable in Figure 6a (top left) due to the relatively small amplitudes (~1 ppmv), is an additional local maximum at low latitudes near 72 km. Local maximums near this altitude region have been found at midlatitudes based on data from the SME [*Thomas*, 1990], referred there as the secondary maximum, and at high latitudes based on the CRISTA data [*Marsh et al.*, 2001; *Kaufmann et al.*, 2003], referred by them as a tertiary maximum. Figure 7 shows ozone (ppmv) zonal mean profiles based on SABER data (years 2002–2005 merged into one 365-day period), from 50 to 90 km, for day 60. The left plot (a) shows our results, which represent averages over longitude and local time from 0 to 20°N latitude, and the right (b) shows results from 28°N to 48°N latitude, but at 16 h local time. Note that the local maximums in 7a and 7b peak at somewhat different altitudes, and as discussed below, are not related. In the right plot (7b), the bulges at midlatitudes compare well with corresponding results from SME [*Thomas*, 1990], as first noted above in reference to Figure 3b. The local maximums in both Figures 7a and 7b are not persistent throughout the year, but have seasonal variations. *Bevilacqua et al.* [1990], and *Marsh and Smith* [2003] have questioned the consistency of the variations of the SME data relative to corresponding water vapor measurements. *Bevilacqua et al.* [1990] noted that the reported semiannual variations of the local maximums in the SME results (which are similar to the local maximums in Figures 3b and 7b between 75 and 80 km and 44°N and 48°N latitude) were not what would be expected based on water vapor variations, which are mostly annual in nature. As discussed earlier with respect to Figure 3, and below with respect to Figure 8 (section 4.2.1), it is possible that the local maximums found in the SME data are due to the local time (~16 h) at which the data were measured, and their semiannual behavior may in part be due to the semiannual variations of the diurnal variations themselves (section 4.2.4).

[30] As for the high latitude local maximums detected near 72 km by CRISTA [*Marsh et al.*, 2001], they were found only at winter latitudes greater than 60°. We do not have results poleward of 48°, so comparisons cannot be made. The local maximums in Figure 7a near 72 km based on SABER data, but at low latitudes, may not be related to the high latitude maximums. *Marsh et al.* [2001] may have missed these variations at low latitudes because the data they used were taken in August, and our results based on SABER data show that the amplitudes appear to follow a semiannual oscillation at low latitudes, and are minimal in August.

4.2. Diurnal Variations

4.2.1. Diurnal Variations With Altitude

[31] The top left (a) plot of Figure 8 shows our derived results based on SABER mixing ratios as a function of local time, from 60 to 70 km, and the top right (b) plot shows the

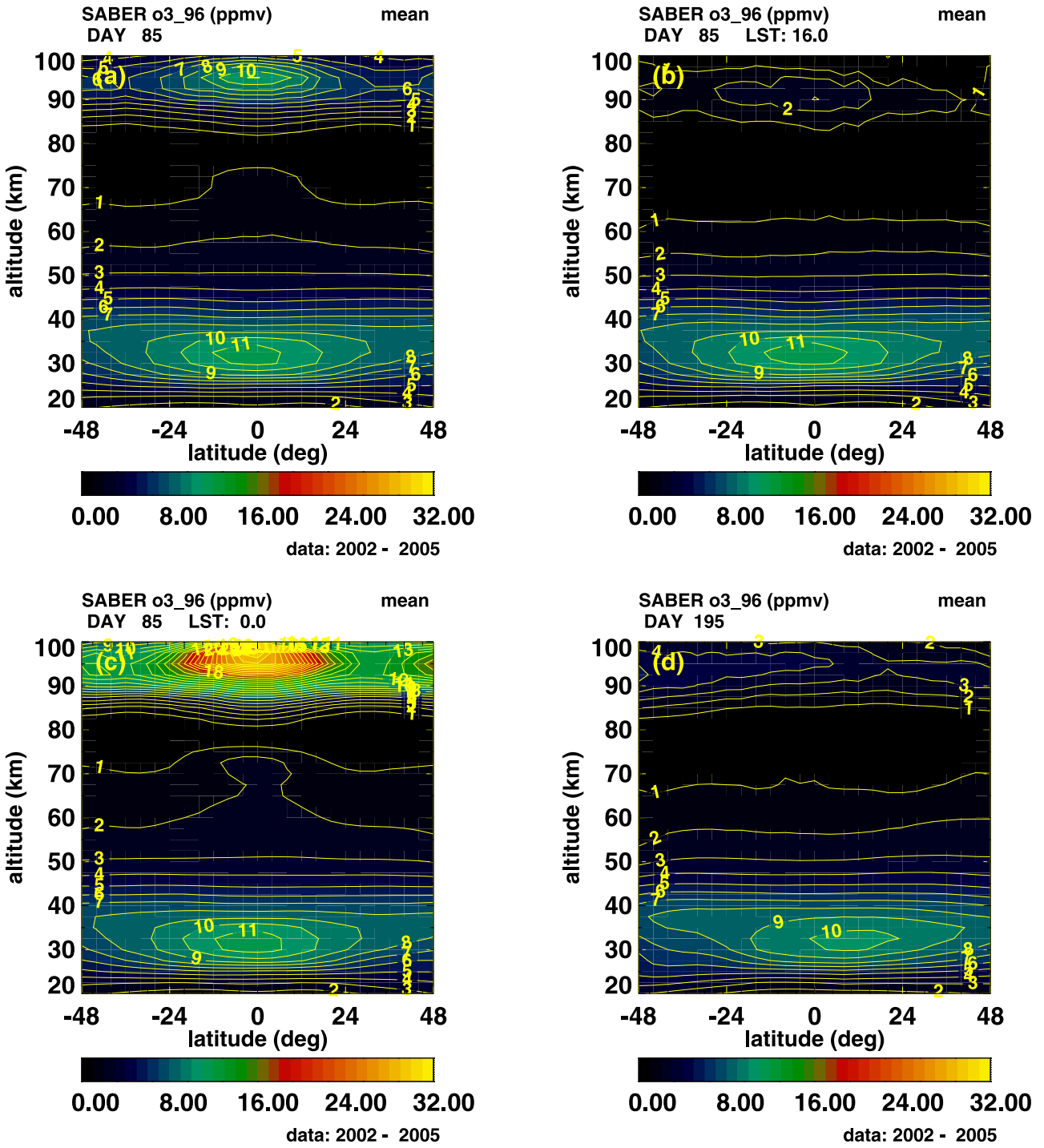

Figure 6. Derived zonal mean ozone mixing ratios (ppmv), based on SABER data for years 2002–2005, on altitude (20 to 100 km) versus latitude (48°S to 48°N) coordinates, for day 85 (upper row (a, b), lower left (c)) and day 195 (lower right (d)). Upper left (a): mean values that are averages over both local time and longitude; upper right (b): corresponds to (a) but at 16 h local time; (c): 12 midnight; (d): corresponds to (a) but for day 195.

corresponding results from 70 to 82.5 km. Each plot corresponds to day 85 at 40°N latitude to represent conditions near equinox. The lower left plot (c) corresponds to the upper right plot (70 to 82.5 km, day 85) but at the Equator, and the lower right plot (d) represents day 195, for conditions near solstice. It can be seen that the magnitude of the changes as a function of local time are generally largest during sunrise (near 6 h) and sunset (near 18 h). They are mostly a result of the reactions

(R1) $$O_3 + h\nu \rightarrow O_2 + O$$

(R2) $$O + O_2 + M \rightarrow O_3 + M$$

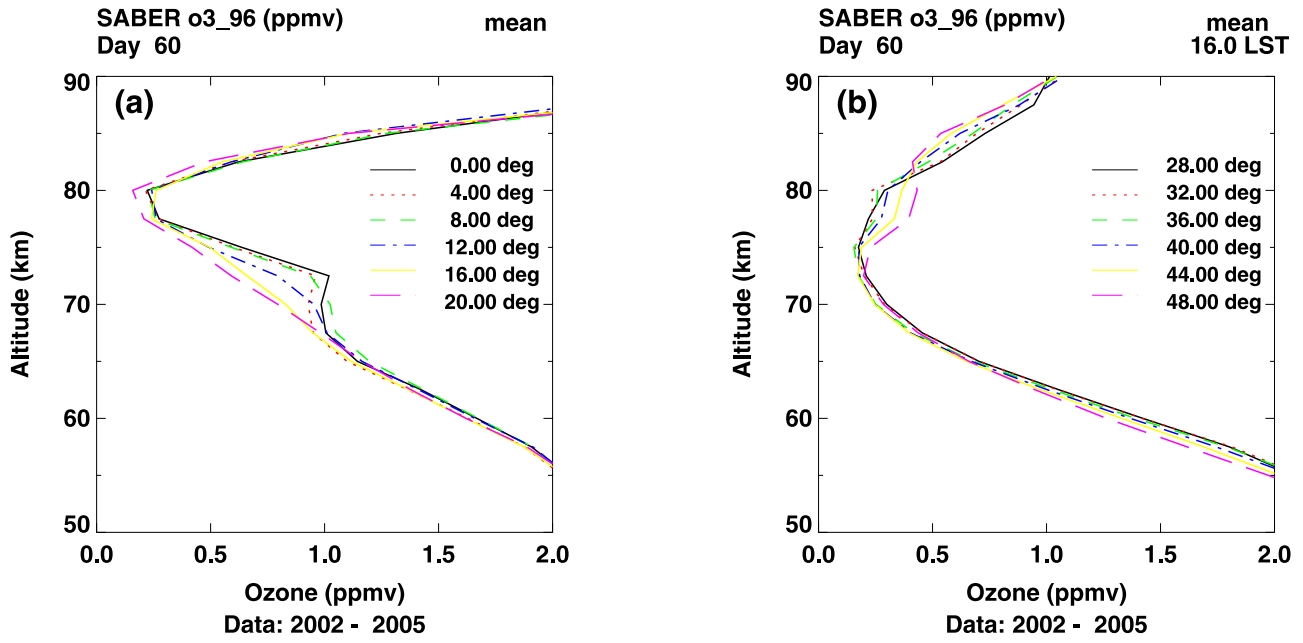

Figure 7. Derived zonal mean ozone mixing ratio (ppmv) profiles based on SABER data. Left (a): mean profiles for day 60 from 0 to 20°N latitude; right (b): from 28°N to 48°N, but at 16 h local time.

which represent the photolysis of ozone (O_3) by solar radiation (R1) and the recombination of molecular (O_2) and atomic (O) oxygen back to ozone (R2). Molecular oxygen is relatively abundant, so the creation of ozone depends largely on the amount of available atomic oxygen.

[32] With the exception of a small altitude range near 80 km, the daytime values are generally smaller than nighttime values. As can be seen in Figure 8, at 77.5 and 80 km, where the ozone mixing ratios are near minimum (as a function of altitude), the daytime values can be larger than the nighttime values. This is consistent with our previous discussion of Figures 3a, and it appears that the bulges at 44°N and 48°N latitude between 75 and 80 km are due to the larger afternoon (near 16 h local time) values at these altitudes. The bulges in our results are no longer apparent for plots of the zonal means that are averages of the ozone over longitude and local time in a consistent manner. As noted before, the ROSE model [*Smith*, 2004, Figure 4] is consistent with our estimates, with the mean nighttime values being smaller than the mean daytime values only near 80 km.

4.2.2. Nighttime Variations

[33] In addition to the larger variations near sunrise and sunset, also discernible in Figure 8 are the post-midnight increases of the ozone mixing ratios. This is not predicted by chemistry alone. For example, *Allen et al.* [1984] estimates that the nighttime density of ozone should be nearly constant from 50 km up to about 80 km since the amount of existing oxygen (and hydrogen) are depleted soon after dusk. *Vaughan* [1984] state that below 65 km, O is almost completely converted to O_3 soon after dusk and the night/day ratio in ozone concentration reflects this balance and also increases with height. However, *Zommerfelds et al.* [1989] have also found post midnight increases using ground-based microwave radiometry measurements over Bern, Switzerland (47°N) from December 1986 through June 1987. They state that the rise in the O_3 mixing ratio by a factor of 2 is a real feature in the data for January 1987 and December 1988, at 66 and 73 km. However, the post midnight increases are not present in their equinoctial (April 1987) data, and are not as prominent in the January/February 1988 data. Also, *Connor et al.* [1994] sees only intermittent increases between midnight and dawn, and not large changes like those measured by *Zommerfelds et al.* [1989]. *Zommerfelds et al.* [1989] surmises that eddy transport may explain this increase. *Huang et al.* [1997] estimated that vertical transport due to thermal tides could account for some of the variations. Our results at 40°N corresponding to day 85 in Figure 8b (top right) show only modest increases in the post midnight values of about 15%, but the increase can be larger at the equator at 70 km, as seen in Figure 8c (lower left), and at higher altitudes (not shown). Because of the coarseness of the altitude resolution (~1.5 O_3 scale height) in their ozone profiles, *Zommerfelds et al.* [1989] present results in relative changes in their differential brightness temperature, so comparison of relative levels of mixing ratios cannot easily be made.

4.2.3. Daytime Variations

[34] As noted earlier, *Marsh et al.* [2002], provide results of daytime diurnal variations based on measurements from HRDI, limited to between about 6 and 18 h local time. They give results from 70 and 82.5 km altitude, near 40°N latitude and also the Equator, for one month beginning in April 1994. Their daytime results (not shown) can be compared with ours in Figure 8 between about 6 to 18 h local time. The overall comparisons are good, although there are also differences. *Marsh et al.* [2002] do not have results before 6 am but their results show the short and persistent increases beginning near 6 AM, similar to our results, especially evident in Figures 8a and 8b. They attribute the initial increase to an increase in O, which rapidly combines with O_2 to form O_3. At 70 and 72.5 km, we both show that these increases are followed by a decrease

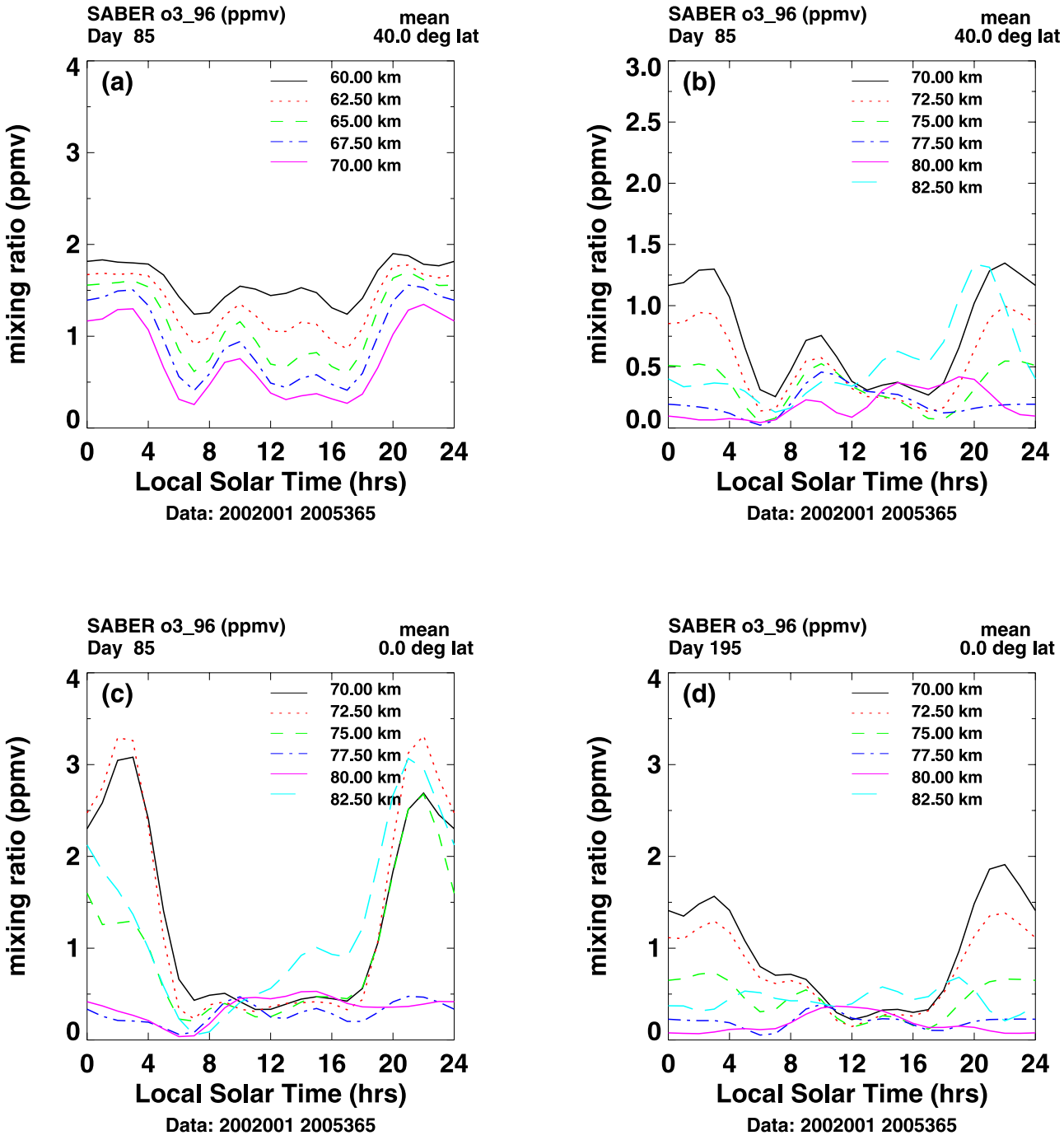

Figure 8. Ozone mixing ratios (ppmv) based on SABER data as a function of local solar time at various altitudes and latitudes. Upper left (a): 60 to 70 km at 40°N latitude, day 85; upper right (b) 70 to 82.5 km at 40°N, day 85; Lower left (c), 70 to 82.5 km at equator, day 85; lower right (d):70 to 82.5 km at equator, day 195.

with local time, and a leveling off in the afternoon. At higher altitudes, we both show a transition, so that at 82.5 km, the larger daytime values are in the afternoon, instead of before 12 h. At 82.5 km we both see a general increase in ozone from about 6 to 15 h LST. Our values are generally higher at the lower altitudes, and are closer at 80 and 82.5 km. We both also show a decrease in daytime mean levels up to about 77.5, with the mean values increasing with altitude near 82.5 km. The main differences between our result and those of Marsh et al. at 40°N between 70 and 82.5 are that our mean levels are larger at the lower altitudes, and we tend to see more local minimums near 12 h (e.g., at 80 km). For example, from Figures 8a and 8b, for 40° latitude, it can be seen that at 70 km, the afternoon daytime values are near 3 ppmv, while the results by *Marsh et al.* [2002] are about 2.6 ppmv, and the differences are within the uncertainties of Marsh's results. The peak near 10 a.m. is more than 0.7 ppmv, while the peak in Marsh's results occurs earlier and only approaches 0.4 ppmv. At 82.5 km, our results start from a low of about 0.15 ppmv at 6 a.m.

and rises to about 0.6 ppmv near 6 p.m., while that of Marsh vary from about 0.2 to 0.5 ppmv, respectively. Again, a visual inspection of the figures shows that the differences are within the uncertainties of *Marsh et al.* [2002], which are generally from 30% to 50%.

[35] At the Equator, the overall agreements are also qualitatively good. At 70 and 72.5 km, we both show local minimums near 12 h. At higher altitudes (80, 82.5 km), we both show a transition to larger mixing ratios in the afternoon. However, this transition is more pronounced in our results, and the local minimums near 12 h are no longer apparent in the results of *Marsh et al.* [2002].

[36] Although the agreement in relative variations in the daylight h is quite good, our mean levels are higher than those of *Marsh et al.* [2002]. As examples, at 70 km and the Equator, the results of *Marsh et al.* [2002] decrease from ~0.36 ppmv near 8 a.m. to ~0.24 ppmv near noon, while our results decrease from 0.6 to 0.25 ppmv. Both level off to ~0.26 ppmv in the afternoon, although there is more structure in Marsh's results. At 82.5 km Marsh's results increase from ~0.18 ppmv near 7 a.m. to about 0.38 ppmv near 4 p.m., peaking at under 0.4 ppmv near 3 p.m., while our results increase from about 0.1 ppmv to about 0.7 ppmv over the same time.

[37] Our algorithm tries to account for seasonal variations and *Marsh et al.* [2002] apparently do not (it takes one month for HRDI to sample the range of day time local times). As seen below when we discuss semiannual oscillations, the seasonal variations are not insignificant relative to the daytime ozone values, especially at the Equator, and there are also other shorter-term variations with season. Because of the SABER viewing geometry, there can be data gaps of varying sizes (~1 h or more) near 12 h local time, and it is possible that some of the local minimums near 12 h, noted earlier, are related to these gaps. We recall that *Marsh et al.* [2002] also show local minimums near 12 h, but they are apparent only at lower altitudes (70–75 km). Even though the results are reasonable, the details might warrant revisiting. We also note that in isolated instances because the day/night differences can be more than an order of magnitude (at high altitudes), relatively small uncertainties in the Fourier estimates can lead to slightly negative values of the near-zero minimum mixing ratios in daytime. This does not appear in any figures presented due to their infrequent occurrence, and although we believe that even in these cases the results are robust in their relative variations, we mention them for the sake of completeness.

4.2.4. Diurnal Variations With Season

[38] Our results show that there are significant seasonal changes in the diurnal variations themselves. From 70 to 80 km, it can be seen from Figure 8 that the diurnal variations are more pronounced at the Equator near equinox (day 85, Figure 8c, lower left) compared to solstice (day 195, Figure 8d, lower right). Figure 9 shows our estimated diurnal and semidiurnal ozone amplitudes (ppmv) for days 85 (top row) and 195 (bottom row), based on SABER data (2002–2005), on altitude (20 to 100 km) versus latitude (48°S to 48°N) coordinates. Although we have estimated 5 Fourier harmonics in local time, the diurnal and semidiurnal components by themselves give a good indication of the overall magnitudes of the variations with local time. It can be seen in Figure 9 that at low latitudes, the amplitudes for day 85 are about twice those for day 195, and that for each of the days, the diurnal amplitudes are about twice those of the semidiurnal amplitudes. Although not shown, corresponding results for days 15 and 270 support the semiannual nature of the variations.

[39] Figure 10 shows the estimated diurnal (left plots) and semidiurnal (right plots) ozone mixing ratio (ppmv) amplitudes on altitude (50 to 85 km) versus day coordinates, based on SABER data from 2002–2005 merged into one 365-day period. Corresponding results based on single year data over these years are qualitatively very similar. The top and bottom rows show results at 0° and 40° latitudes, respectively. At the equator, the diurnal variations follow more of a semiannual variation, with local maximums that are near equinox, and near 72 and 95 km in altitude. At 40°, the diurnal amplitudes appear to follow more of an annual variation below about 75 km, while the behavior of the semidiurnal components depends more on the altitude. Because the seasonal variations of the diurnal variations themselves are not negligible compared to the mean seasonal variations, their effects on the interpretation of seasonal effects should be considered. Although not shown, the estimates of the semiannual oscillation (SAO) amplitudes in ozone are a ~few tenths ppmv [*Huang et al.*, 2008]. For example, the SME data, which are all measured near 16 h local time, would contain the seasonal variations of the diurnal variations as well, in addition to those of the mean variations (not shown).

5. Summary and Discussion

[40] We have derived global ozone diurnal variations (over 24 h local time) and mean profiles, based on zonal mean SABER data, as a function of altitude (20–100 km), latitude (48°S to 48°N), and day (over an annual cycle). In the MLT, these comprehensive results have not been heretofore available.

5.1. Advantages of Saber Data

[41] Ozone and temperature measurements from SABER are unique in the breadth of their information content. Measurements are made over the globe from about 15 to 100 km, over 24 h in local solar time (LST), since the beginning of 2002. This kind of comprehensive information has not been available previously, especially from one instrument. SABER data provide the potential to realistically estimate global diurnal variations up to 100 km, and the behavior of the diurnal variations themselves over an annual cycle.

5.2. Analysis

[42] For a given day and latitude, the measurements all correspond to one local time, and it takes 60 days for SABER to sample over the 24 h of local time. Over 60 days, variations can be due to both local time and other variables, such as season. Diurnal and mean variations are embedded together in the data, and need to be unraveled from each other to obtain more accurate estimates of each. The algorithm is designed for this type of sampling, and identifies the separate variations to provide diurnal variations throughout the year and mean variations such as semiannual (SAO) and quasi-biennial (QBO) oscillations of ozone and

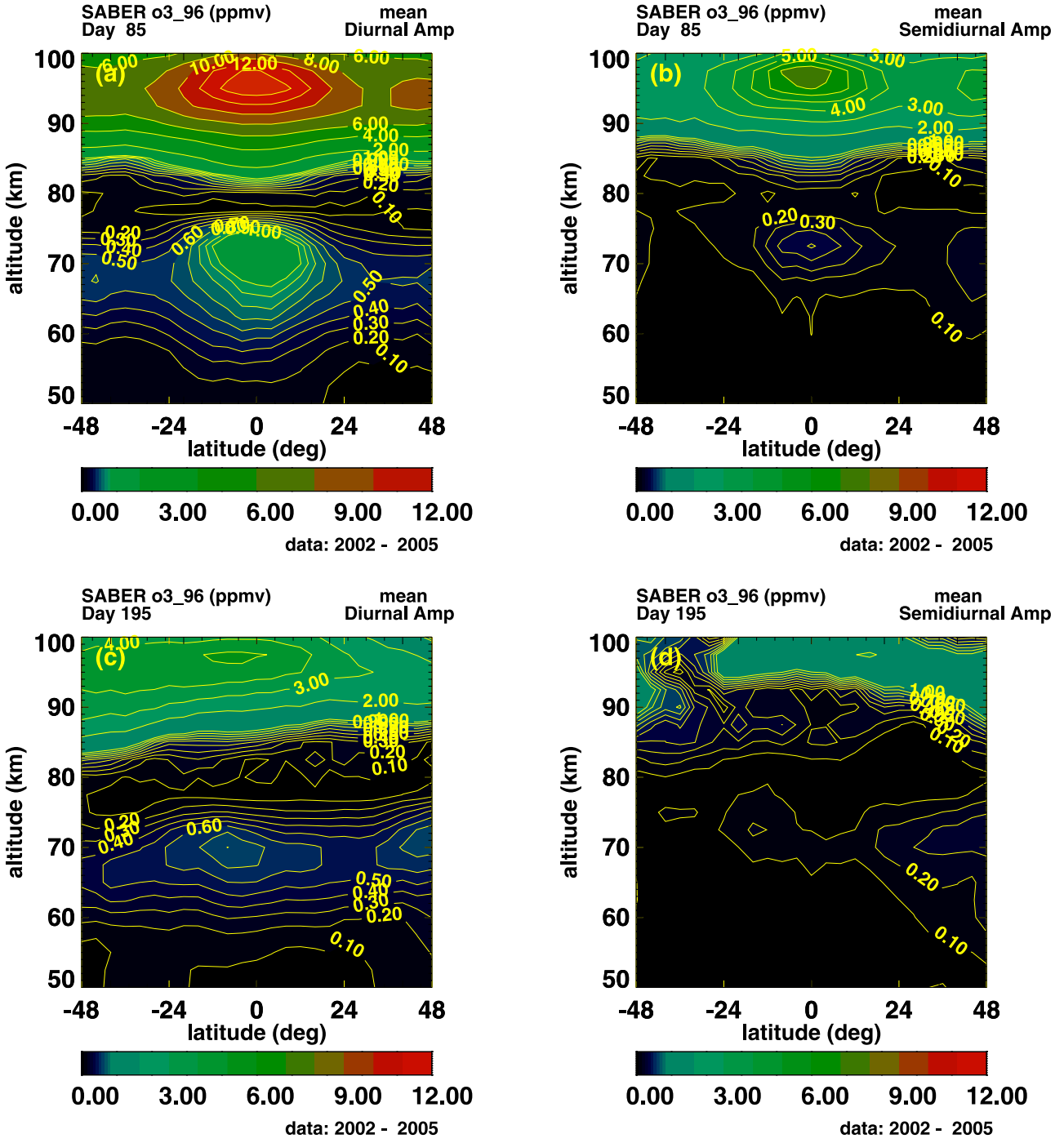

Figure 9. Estimated diurnal (left plots) and semidiurnal (right plots) ozone mixing ratio (ppmv) amplitudes for days 85 (top row) and 195 (bottom row), based on SABER data (2002–2005), on altitude (50 to 100 km) versus latitude (48°S to 48°N) coordinates.

temperature. The QBO and SAO for temperatures were first given by *Huang et al.* [2006c], and those for ozone are the subjects of a companion paper [*Huang et al.*, 2008]. For this study, the correlations between the ozone and temperature QBO are given in Figure 5, and lend support to the validity of the data, as discussed in the text and below.

5.3. Data Quality

[43] From the middle mesosphere to higher altitudes, departures from local thermodynamic equilibrium (non-LTE) can be significant, thereby complicating the retrieval process to obtain ozone mixing ratios, and the uncertainties can be larger than those at lower altitudes. Comparisons among measurements from various sources in the literature of upper mesosphere and lower thermosphere ozone are mostly not fruitful in reaching definite conclusions. Fortunately, experience indicates that measurements of relative variations from a mean state, such as diurnal variations, the QBO, and SAO, are more robust. However, we do not assume such is the case, and our

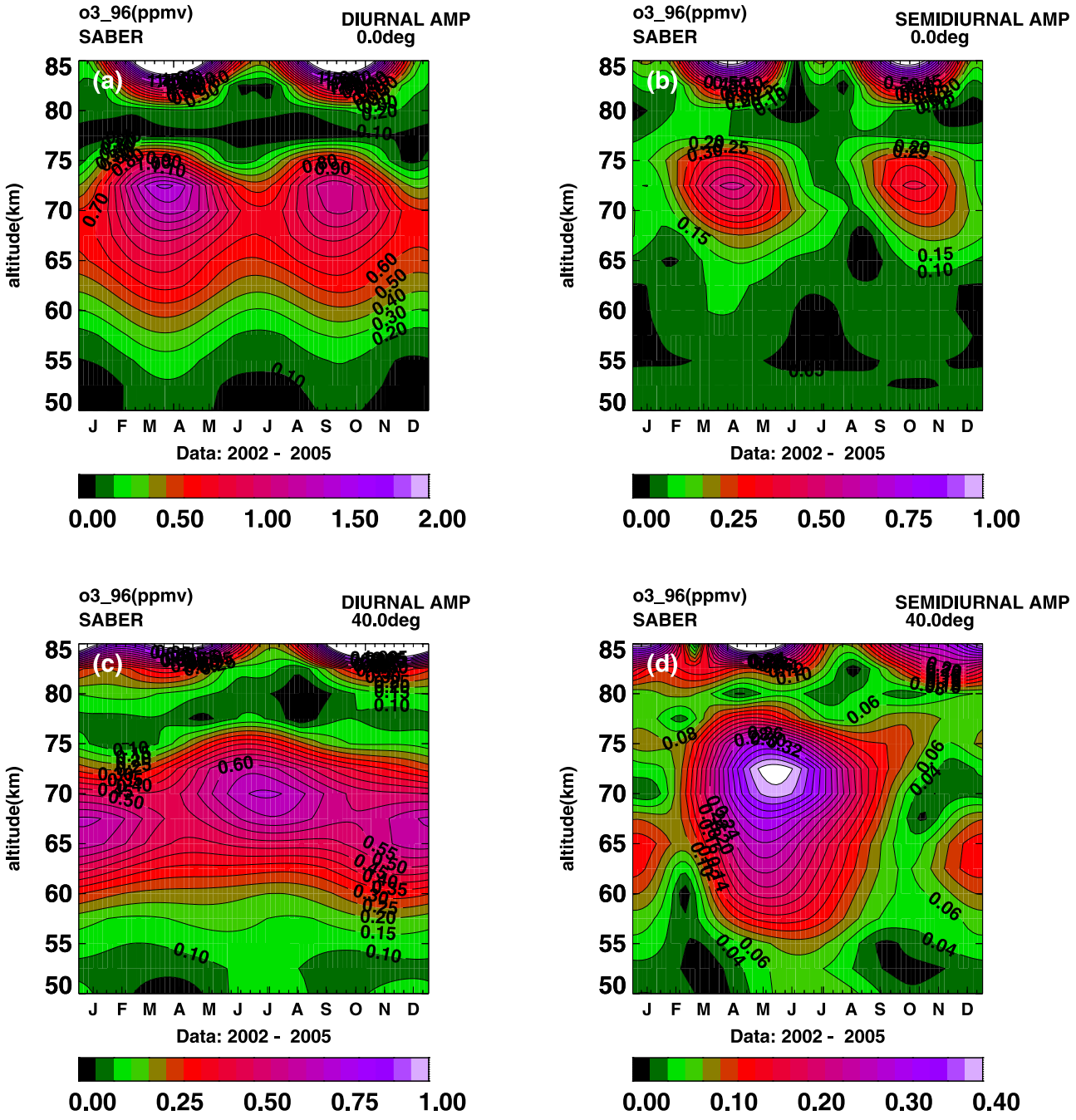

Figure 10. Estimated diurnal (left plots) and semidiurnal (right plots) ozone mixing ratio (ppmv) amplitudes on altitude (50 to 85 km) versus day coordinates, based on SABER data (2002–2005). Top row: 0° latitude, lower row: 40°.

approach has been to examine these variations based on the sensitivity of relative changes, as in Figures 3, 4, 5, and 8. The sensitivity of the SABER data to relatively small changes are clearly shown in both Figures 3a and 3b near 80 km, especially in the good agreement of 3a with the ROSE model [*Smith*, 2004, Figure 4] and 3b with the SME data [*Thomas*, 1990]. As noted earlier in Figure 3, the likelihood of (a) the bulges being in both the SME and in our results between 75 and 80 km, (b) the ozone daytime concentration being larger than the nighttime concentration only near 80 km, and (c) the agreement of (b) with the ROSE model all being coincidental is obviously low. In Figure 4, we have compared results based on SABER measurements with that from MLS measurements. In the transition region, these relative variations show agreement to a few percent.

[44] That the algorithm estimates the QBO and SAO in conjunction with the diurnal variations is the subject of a companion paper [*Huang et al.*, 2008]. Although not the focus of this study, Figure 5 shows a sample of the ozone and temperature QBO to underscore further the validity of the SABER data and the analysis. In the stratosphere, where

there are more abundant measurements with which to compare, the comparisons are very good, including the ozone QBO phase change with altitude near 29–31 km, which has been previously attributed to the change in control of dynamics versus chemistry. At higher altitudes, our comparisons of QBO ozone with corresponding temperature results not only provide new information, they show the continued phase relations between the ozone and temperature QBO from the stratosphere into the MLT. It is unlikely that the observed extension of the expected phase relationships from the stratosphere into the mesosphere (and higher) is fortuitous.

5.4. Results of Diurnal Variations

[45] We have derived diurnal variations and mean profiles of ozone mixing ratios as a function of altitude (20–100 km), latitude (48°S to 48°N), and day, over an annual cycle. Diurnal variations of ozone can be significant from the upper stratosphere into the mesosphere and lower thermosphere, and our comprehensive results in these regions are essentially new. Previous measurements do not have the combined spatial and temporal coverage that SABER provides.

[46] We have also compared diurnal variations over 24 h in local time with previous measurements in relation to Figure 8. Generally, diurnal variations over 24 h of local time display (1) post-midnight increases, followed by (2) decreases near sunrise, (3) short persistent increases that follow the sunrise decrease, (4) variable behavior during daytime, and (5) increases near sunset. There are scant measurements by one instrument with which to compare over the 24 h of local time. However, piecewise comparisons with various measurements support the findings of (1) through (5), above. Some of the piecewise variations are relatively small, further supporting sensitivity of the results. *Zommerfelds et al.* [1989] suggest transport as the cause for the post-midnight increase in ozone.

5.4.1. Diurnal Variations as a Function of Altitude and Latitude

[47] The magnitudes of the ozone diurnal variations increase with altitude from the upper stratosphere into the lower mesosphere, then decrease until about 80 km in altitude, and increase again into the lower thermosphere. At low latitudes, the diurnal amplitudes show peaks near 72 and 95 km, while the averages over local time exhibit local maximums near 30, 72, and 95 km. In a small altitude range near 80 km, unlike the case at other altitudes, the mean daytime ozone mixing ratios can be larger than the nighttime values. As discussed above in reference to Figure 3b, it appears that this may be the origin of the bulges between 75 and 80 km, near 45°N, in both this work and the SME results, since the mixing ratios are larger near 16 h local time (at which SME samples all data). These results are essentially new. For the mean profiles, *Kaufmann et al.* [2003] suggest that the equatorial maximum near 95 km is likely because of downward transport of atomic oxygen due to atmospheric tides (based on the ROSE model [*Rose and Brasseur*, 1989]), and the latitudinal distribution is also strongly biased by thermal tides.

5.4.2. Diurnal Variations as a Function of Season

[48] In addition to being functions of altitude, the magnitudes of the diurnal variations also display seasonal variations, and tend to be larger at equatorial latitudes than at midlatitudes. At low latitudes, the diurnal variations follow more of a semiannual variation, with local maximums that are near equinox, and 72 and 95 km in altitude. For midlatitudes, the diurnal amplitudes appear to follow more of an annual variation below about 75 km, while the behavior of the semidiurnal components depends more on the altitude. The ozone mean SAO therefore needs to be interpreted in conjunction with the semiannual variations of the diurnal variations themselves.

Appendix A: Data Analysis Algorithm

[49] For a given latitude and altitude, the algorithm performs a two-dimensional Fourier least squares analysis in the form

$$\Psi(t_l, d, z, \theta, \lambda) = \sum_n \sum_k b_{nk}(z, \theta, \lambda) e^{i2\pi n t_l} e^{i2\pi k d/N} \quad \text{(A1)}$$

where $\Psi(t_l, d, z, \theta, \lambda)$ represents the input data; z is altitude; d is day of year; θ latitude; λ longitude (radians); t_l = local solar time (fraction of a day) = $t + \lambda/2\pi$; t = time of day (fraction of day), and N is the number of days in the fundamental period. For example, if we analyze data over one year, then N = 365.

[50] In this study, we apply the algorithm to data averaged over longitude, although it has been applied to data with longitude variations as well [*Huang and Reber*, 2004]. For variations with longitude, we use data at discrete longitudes $\{\lambda_l\}$ to find the set $b_{nk}(z, \theta, \lambda_i)$ from (A1). To analyze the behavior with longitude, we estimate $\alpha_{mnk}(z, \theta)$ from

$$b_{nk}(z, \theta, \lambda_i) = \sum_m \alpha_{mnk}(z, \theta) e^{i2\pi m \lambda_i/2\pi} \quad \text{(A2)}$$

again using a least squares fit. Finally, for any day of year d_0, we can sum (A1) over k to obtain

$$\Psi(t_l, d_0, z, \theta, \lambda) = \sum_m \sum_n \beta_{nm}(z, \theta) e^{i2\pi m \lambda/2\pi} e^{i2\pi n t} \quad \text{(A3)}$$

where we use β_{nm} to denote the transform to universal time t (fraction of a day).

[51] If we average the data over longitude, then we obtain the migrating diurnal variations and mean flows [*Huang and Reber*, 2004] from (A1), where the coefficients are no longer dependent on λ. Once we have estimated the coefficients in (A1) or (A3), we can directly generate the diurnal variations for composition, winds, and temperature as a function of day of year, longitude, and time. TIMED sampling patterns are such that data at latitudes poleward of about 50° are made only for alternate yaw periods. Therefore our current analyses are made only within 48° of the Equator.

[52] Our fits to the data are based on data over a period of one year or more. Currently in (A1), the maximum value of n is 5 for ozone, and the maximum of k depends on the fundamental period in day of year. Because it takes SABER 60 days to sample over the range of local times, when the fundamental day-of-year period is 365 days, we estimate the coefficients $b_{nk}(z, \theta, \lambda_i)$ for k greater than or equal to 3 only for n = 0, and the maximum of k is 6. When the fundamental period corresponds to the QBO, the number of terms for day-of-year is scaled up accordingly. The current version of the data does not provide for uncertainties, and we also

assume that the uncertainties of the data are proportional to the data values themselves.

[53] **Acknowledgments.** We thank two anonymous reviewers for their insightful comments.

[54] Zuyin Pu thanks the reviewers for their assistance in evaluating this paper.

References

Allen, M., J. I. Lunine, and Y. L. Yung (1984), The vertical distribution of ozone in the mesosphere and lower thermosphere, *J. Geophys. Res.*, *89*, 4841–4872.

Barth, C. A., D. W. Rusch, R. J. Thomas, G. H. Mount, G. J. Rottman, G. E. Thomas, R. W. Sanders, and G. M. Lawrence (1983), Solar mesosphere explorer: Scientific objectives and results, *Geophys. Res. Lett.*, *10*, 237–240, April.

Bevilacqua, R. M., D. F. Strobel, M. E. Summers, J. J. Olivero, and M. Allen (1990), The seasonal variation of water vapor and ozone in the upper mesosphere: Implications for vertical transport and ozone photochemistry, *J. Geophys. Res.*, *95*(D1), 883–893.

Boyd, I. S., A. D. Parrish, L. Froidevaux, T. von Clarmann, E. Kyrola, J. M. Russell III, and J. M. Zawodny (2007), Ground-based microwave ozone radiometer measurements compared with Aura-MLS v2.2 and other instruments at two Network for Detection of Atmospheric Composition Change sites, *J. Geophys. Res.*, *112*, D24S33, doi:10.1029/2007JD008720.

Brasseur, G. P., and S. Solomon (2005), *Aeronomy of the Middle Atmosphere, Chemistry and Physics of the Stratosphere and Mesosphere*, Springer, Dordrecht, The Netherlands.

Connor, B. J., D. E. Siskind, J. J. Tsou, A. Parrish, and E. E. Remsberg (1994), Ground-based microwave observations of ozone in the upper stratosphere and mesosphere, *J. Geophys. Res.*, *99*, 16,757–16,770, August.

Douglass, A., R. B. Rood, and R. S. Stolarski (1985), Interpretation of ozone temperature correlations 2. Analysis of SBUV ozone data, *J. Geophys. Res.*, *90*, 10,693–10,708, October.

Finger, F. G., R. M. Nagatani, M. E. Gelman, C. S. Long, and A. J. Miller (1995), Consistency between variations of ozone and temperature in the stratosphere, *Geophys. Res. Lett.*, *22*, 3477.

Froidevaux, L., et al. (2007), Validation of Aura Microwave Limb Sounder stratospheric ozone measurements, *J. Geophys. Res.*, *112*, D24534, doi:10.1029/2007JD008776.

Hasebe, F. (1994), Quasi-biennial oscillations of ozone and diabatic circulation in the equatorial stratosphere, *J. Atmos. Sci.*, *51*, 729–745, March.

Hollandsworth, S. M., K. P. Bowman, and R. D. McPeters (1995), Observational study of the quasi-biennial oscillation in ozone, *J. Geophys. Res.*, *100*, 7347–7361, April.

Huang, F. T., and C. A. Reber (2004), Non-migrating semidiurnal and diurnal tides at 95 km, based on wind measurements from the high resolution Doppler imager (HRDI) on the Upper Atmosphere Research Satellite (UARS), *J. Geophys. Res.*, *109*, D10110, doi:10.1029/2003JD004442.

Huang, F. T., C. A. Reber, and J. Austin (1997), Ozone diurnal variations observed by UARS and their model simulation, *J. Geophys. Res.*, *102*, 12,971–12,985.

Huang, F. T., H. G. Mayr, C. A. Reber, T. Killeen, J. Russell, M. Mlynczak, W. Skinner, and J. Mengel (2006a), Diurnal variations of temperature and winds inferred from TIMED and UARS measurements, *J. Geophys. Res.*, *111*, A10S04, doi:10.1029/2005JA011426.

Huang, F. T., H. G. Mayr, C. A. Reber, J. M. Russell, M. Mlynczak, and J. Mengel (2006b), Zonal-mean temperature variations inferred from SABER measurements on TIMED compared with UARS observations, *J. Geophys. Res.*, *111*, A10S07, doi:10.1029/2005JA011427.

Huang, F. T., H. G. Mayr, C. A. Reber, J. M. Russell, M. Mlynczak, and J. Mengel (2006c), Stratospheric and mesospheric temperature variations for the quasi-biennial and semiannual (QBO and SAO) oscillations based on measurements from SABER (TIMED) and MLS (UARS), *Ann. Geophys.*, *24*, 2131–2149.

Huang, F. T., H. G. Mayr, C. A. Reber, J. M. Russell III, M. G. Mlynczak, and J. Mengel (2008), Ozone quasi-biennial oscillations (QBO), semi-annual oscillations (SAO), and correlations with temperature in the mesosphere, lower thermosphere, stratosphere, based on measurements from SABER on TIMED and MLS on UARS, *J. Geophys. Res.*, *113*, A01316, doi:10.1029/2007JA012634.

Kaufmann, M., O. A. Gusev, K. U. Grossmann, F. J. Martin-Torres, D. R. Marsh, and A. A. Kutepov (2003), Satellite observations of daytime and nighttime ozone in the mesosphere and lower thermosphere, *J. Geophys. Res.*, *108*(D9), 4272, doi:10.1029/2002JD002800.

Marsh, D., and A. Smith (2003), Mesopheric ozone response to changes in water vapor, *J. Geophys. Res.*, *108*(D9), 4109, doi:10.1029/2002JD002705.

Marsh, D. R., A. Smith, G. Brasseur, M. Kaufmann, and K. Grossmann (2001), The existence of a tertiary ozone maximum in the high-latitude middle mesosphere, *Geophys. Res. Lett.*, *28*, 4531–4534.

Marsh, D. R., W. R. Skinner, A. R. Marshall, P. B. Hays, D. A. Ortland, and J. H. Yee (2002), High Resolution Doppler Imager observations of ozone in the mesosphere and lower thermosphere, *J. Geophys. Res.*, *107*(D9), 4390, doi:10.1029/2001JD001505.

Reber, C. A. (1993), The Upper Atmosphere Research Satellite (UARS), *Geophys. Res. Lett.*, *20*(12), 1215–1218.

Ricaud, P., J. De La Noe, B. J. Connor, L. Froidevaux, J. W. Waters, R. S. Harwood, I. A. MacKenzie, and G. E. Peckham (1996), Diurnal Variability of mesospheric ozone as measured by the UARS microwave limb sounder instrument: Theoretical and ground based validations, *J. Geophys. Res.*, *101*, 10,077–10,089, April.

Rood, R. B., and A. Douglass (1985), Interpretation of ozone temperature correlations 1. Theory, *J. Geophys. Res.*, *90*, 5733–5743, June.

Rose, K., and G. Brasseur (1989), A three dimensional model of chemically active trace species in the middle atmosphere during disturbed winter conditions, *J. Geophys. Res.*, *94*, 16,387–16,403.

Russell, J. M., III, M. G. Mlynczak, L. L. Gordley, J. Tansock, and R. Esplin (1999), An overview of the SABER experiment and preliminary calibration results, in *Proceedings of the SPIE, 44th Annual Meeting, Denver, Colorado, July 18–23*, *3756*, pp. 277–288.

Schneider, N., F. Selsis, J. Urban, O. Lezeaux, J. DelaNoe, and P. Ricaud (2005), Seasonal and diurnal ozone variations: Observations and modeling, *J. Atmos. Chem.*, *50*, 25–47.

Smith, A. (2004), Physics and chemistry of the mesopause region, *J. Atmos. Sol. Terr. Phys.*, *66*, 839–857, July.

Thomas, R. J. (1990), Seasonal ozone variations in the upper mesosphere, *J. Geophys. Res.*, *95*, 7395–7401, May.

Vaughan, G. (1984), Mesospheric ozone - Theory and observation, *Q. J. R. Meteorol. Soc.*, *110*, 239–260.

Wu, D. L., and J. H. Jiang (2005), Interannual and seasonal variations of diurnal tide, gravity wave, ozone, and water vapor as observed by MLS during 1991–1994, *Adv. Space Res.*, *35*, 1999–2004.

Zommerfelds, W. C., K. F. Kunzi, M. E. Summers, R. M. Bevilacqua, D. F. Strobel, M. Allen, and W. J. Sawchuck (1989), Diurnal variations of mesospheric ozone obtained by ground-based microwave radiometry, *J. Geophys. Res.*, *94*, 12,819–12,832, September.

F. T. Huang, Creative Computing Solutions Inc., 1901 Research Boulevard, Rockville, MD 20850, USA. (fthuang@comcast.net)

H. G. Mayr, NASA Goddard Space Flight Center, Greenbelt, MD 20771, USA.

M. G. Mlynczak, NASA Langley Research Center, Hampton, VA 23681, USA.

C. A. Reber, Science and Technology Corporation, Hampton, VA 23666, USA.

J. M. Russell III, Center for Atmospheric Sciences, Hampton University, Hampton, VA 23668, USA.